

Feedback control of subcritical oscillatory instabilities

A. A. Golovin¹ and A. A. Nepomnyashchy²

¹*Department of Engineering Sciences and Applied Mathematics, Northwestern University, Evanston, Illinois 60208, USA*

²*Department of Mathematics and Minerva Center for Physics of Complex Systems, Technion-Israel Institute of Technology, Haifa 32000, Israel*

(Received 26 October 2005; published 28 April 2006)

Feedback control of a subcritical oscillatory instability is investigated in the framework of a globally-controlled complex Ginzburg-Landau equation that describes the nonlinear dynamics near the instability threshold. The control is based on a feedback loop between the system linear growth rate and the maximum of the amplitude of the emerging pattern. It is shown that such control can suppress the blow up and result in the formation of spatially localized pulses similar to oscillons. In the one-dimensional case, depending on the values of the linear and nonlinear dispersion coefficients, several types of the pulse dynamics are possible in which the computational domain contains: (i) a single stationary pulse; (ii) several coexisting stationary pulses; (iii) competing pulses that appear one after another at random locations so that at each moment of time there is only one pulse in the domain; (iv) spatiotemporally chaotic system of short pulses; (v) spatially-synchronized pulses. Similar dynamic behavior is found also in the two-dimensional case. The effect of the feedback delay is also studied. It is shown that the increase of the delay leads to an oscillatory instability of the pulses and the formation of pulses with oscillating amplitude.

DOI: [10.1103/PhysRevE.73.046212](https://doi.org/10.1103/PhysRevE.73.046212)

PACS number(s): 82.40.Bj, 89.75.Kd, 47.54.-r

I. INTRODUCTION

Numerous physical, chemical, and biological systems far from equilibrium exhibit oscillatory instabilities that are characterized by the appearance of waves and other oscillating patterns [1]. If the instability is supercritical, its nonlinear dynamics is described by a complex Ginzburg-Landau equation (CGLE) that exhibits a great plethora of spatiotemporal patterns that was studied extensively over the years [2]. In the case of a *subcritical* oscillatory instability, the system dynamics cannot usually be described by an amplitude equation such as CGLE, since the absence of nonlinear saturation at the cubic order drives the system out of the weakly nonlinear regime. Although for certain values of the dispersion and Landau coefficients a subcritical CGLE still has bounded solutions [3,4] (as well as CGLE with the pure imaginary Landau coefficient [5]), in most of cases its solutions blowup in a finite time which corresponds to the transition of the system dynamics to a strongly nonlinear regime beyond the applicability of CGLE. In many cases, however, such strong growth of perturbations near a subcritical instability threshold is undesirable. In this paper, we show that the blowup of weakly nonlinear solutions in subcritical CGLE can be suppressed by means of feedback control which allows one to keep the system dynamics in a weakly nonlinear regime, when the amplitude of perturbations remains small.

Feedback control of instabilities and nonlinear dynamics in systems far from equilibrium has been attracting growing attention. It has been shown that it can be applied to Rayleigh-Benard convection [6–9], Marangoni convection [10–12], contact line instability in thin liquid films [13], excitable media [14–17], and other reaction-diffusion systems [18], catalytic reactions [19,20], and crystal growth [21,22]. The effect of feedback control on nonlinear dynamics of a supercritical oscillatory instability described by a CGLE with additional, global feedback control term with delay, was in-

vestigated in [23–25] in one- (1D) and two-dimensional cases. It was shown that, by adjusting the feedback intensity and the delay time, one can destroy the phase slips and spiral waves, and produce breathing and stationary cellular structures. Similar equation with global delayed feedback control was analyzed recently in relation to spatiotemporal control of cardiac alternans [26]. In a recent work [27] a controlled, one-dimensional CGLE with spatiotemporally delayed control term was considered; it was shown that delayed feedback control can stabilize traveling waves for the parameters outside the Benjamin-Feir stability region. Similar conclusion was made in [28] for feedback control of a 1D oscillatory convection pattern described by a CGLE.

In the above examples feedback control of only supercritical oscillatory instabilities was investigated. A possibility to control and suppress the blow up behavior caused by *subcritical* oscillatory instability, to the best of our knowledge, has not been studied. In the present paper we report the results of our investigation of feedback control of systems characterized by a subcritical oscillatory instability.

II. MODEL

Consider a system that exhibits a subcritical oscillatory instability at a finite wave number characterized, near the instability threshold, by a dispersion relation $\sigma(k) = \gamma + i\omega$, $\gamma = \gamma_R(R - R_c) - \delta(k - k_c)^2 + \dots$, $\omega = \omega_0 + \omega_1(k - k_c) + \omega_2(k - k_c)^2 + \omega_R(R - R_c) + \dots$, where σ is the growth rate of perturbations with the wave number k , R is a bifurcation parameter, k_c is the wave number corresponding to the instability threshold, R_c , and $R - R_c = O(\epsilon^2)$, $k - k_c = O(\epsilon)$, $\epsilon \ll 1$. Consider a *feedback control* of the bifurcation parameter that will put the supercriticality in the following feedback loop with the perturbation complex amplitude, A

$$R - R_c = \epsilon^2(1 - P \max|A|), \quad (1)$$

where the maximum is computed over the whole domain. In experiment, such feedback control could be implemented by adjusting, e.g., the temperature difference across the liquid layer in Rayleigh-Benard or Marangoni convection system [9], by controlling the pulling speed in directional solidification [22], by tuning the external pressure and temperature in catalytic systems [19,20], by changing the illumination intensity in light-sensitive reaction-diffusion systems [14–17], etc. Of course, measuring the perturbation amplitude in a physical experiment will require certain time, especially if the pattern evolves in a large domain, so that, generally, one should take into account the time delay between the action of sensors and actuators in such an experiment and consider

$$R - R_c = \epsilon^2[1 - P \max|A(t - \tau)|], \quad (2)$$

where τ is the delay time. At the same time, in some cases the typical time delay can be small in comparison with the characteristic time of the pattern evolution, and the feedback delay can be neglected or it will not lead to a qualitative change of the system behavior. We first concentrate on the case when the feedback delay can be neglected, and discuss the effect of delay in the last section of the paper.

Thus, we consider the feedback control of a bifurcation parameter (1). In this case the nonlinear dynamics near the instability threshold will be described by a CGLE with an additional control term; after appropriate rescaling, the controlled CGLE will have the following form:

$$A_t = A + (1 + i\alpha)A_{xx} + (1 + i\beta)|A|^2A - pA \max|A|, \quad (3)$$

where p is the rescaled control parameter, $p \propto (\gamma_R + i\omega_R)P$. Note, however, that using the transformation $\arg(A) \rightarrow \arg(A) + \text{Im}(p) \int_0^t \max_x |A(s)| ds$, one can eliminate $\text{Im}(p)$ from Eq. (3). Thus, we shall further consider the control parameter p to be *real* and positive.

III. TRAVELING WAVE SOLUTIONS

Equation (3) has two traveling wave (TW) solutions

$$\begin{aligned} A &= R_{\pm} \exp[i(kx - \Omega t)], \\ R_{\pm} &= p/2 \pm \sqrt{p^2/4 - 1 + k^2}, \\ \Omega &= \alpha k^2 - \beta R_{\pm}^2, \end{aligned} \quad (4)$$

for $p > 2\sqrt{1-k^2}$, one TW solution, $A = R_{+} \exp[i(kx - \Omega t)]$, for $|k| > 1$, and no TW solutions for $p < 2\sqrt{1-k^2}$. However, all TW solutions (4) are unstable. In order to demonstrate this, consider $A = (R_{\pm} + \tilde{R}) \exp[i(kx - \Omega t + \tilde{\theta})]$ and linearize Eq. (3) with respect to perturbations \tilde{R} and $\tilde{\theta}$. First consider spatially homogeneous perturbations, $\tilde{\theta} = 0$, $\tilde{R} = \bar{R} e^{\sigma t}$. From the linearized equation for \tilde{R} one obtains $\sigma_0 = \partial F(R_{\pm}) / \partial R_{\pm}$, where $F(x) = x[x^2 - px + (1 - k^2)]$. One can readily see that the TW solution with R_{+} is always unstable, while the TW solution with R_{-} is stable with respect to spatially homogeneous perturbations for $|k| < 1$, $p > 2\sqrt{1-k^2}$. In order to study the sta-

bility of the TW solutions with respect to spatially-periodic perturbations, consider $\tilde{R} = \text{Re}(\hat{R} e^{iqx + \sigma t}) + \tilde{R}_0(t)$, $\tilde{\theta} = \text{Re}(\hat{\theta} e^{iqx + \sigma t}) + \tilde{\theta}_0(t)$, where the spatially-homogeneous parts of the perturbations, $\tilde{R}_0(t)$ and $\tilde{\theta}_0(t)$, must be added due to the presence of the control term in Eq. (3) that results in a nonlocal term $p(\max \tilde{R})R_{\pm}$ in the equation for \tilde{R} . However, this term contributes only to the spatial average of the perturbation, $\langle \tilde{R} \rangle$, and therefore, the evolution of $\tilde{R}_0(t)$ and $\tilde{\theta}_0(t)$ is decoupled from the evolution of the spatially-periodic parts of the perturbations characterized by the amplitudes \hat{R} and $\hat{\theta}$. Thus, from the linearized equations one obtains the following dispersion relation:

$$\begin{aligned} \sigma^2 + \sigma[2(q^2 - R_{\pm}^2) + 4iakq] + q^2(1 + \alpha^2)(q^2 - 4k^2) \\ - 2R^2q[q(1 + \alpha\beta) + 2ik(\alpha - \beta)] = 0. \end{aligned} \quad (5)$$

For $q \rightarrow 0$, Eq. (5) has the root $\sigma = 2R_{\pm}^2 > 0$. Therefore, all traveling waves (4) are unstable with respect to long-wave amplitude modulations.

IV. PULSE SOLUTIONS

Besides traveling wave solutions, the subcritical CGLE with control (3) has the following *pulse* solutions:

$$A_p(x, t) = R_p(x) e^{-i\Theta_p(x, t)}, \quad (6)$$

$$R_p(x) = \frac{a_p}{\cosh \kappa_p x}, \quad \Theta_p = \gamma_p \ln \cosh \kappa_p x + \Omega_p t,$$

where

$$\begin{aligned} a_p &= (pY/2)[1 \pm \sqrt{1 - 4/(p^2Y)}], \\ Y &= \frac{3[9 + 8\alpha^2 + \alpha\beta + \sqrt{9(1 + \alpha\beta)^2 + 8(\alpha - \beta)^2}]}{2(9 + 8\alpha^2 + 2\alpha\beta - \beta^2)}, \\ \kappa_p^2 &= a_p^2 \left[\frac{3 + \alpha\beta + 2\alpha^2}{3(1 + \alpha^2)} - \frac{1}{Y} \right], \end{aligned} \quad (7)$$

$$\gamma_p = \frac{\alpha - \beta}{3 + \alpha\beta + 2\alpha^2 - 3(1 + \alpha^2)Y},$$

$$\Omega_p = \kappa_p^2 [2\gamma_p + \alpha(\gamma_p^2 - 1)].$$

Solution (6) and (7), is analogous to the well-known Nozaki-Bekki solution of a supercritical CGLE [29]; see also [2,30] for review. Similar pulse solutions were studied for a subcritical cubic CGLE in [3,4] and for a subcritical quintic CGLE in [31,32].

For $Y > 0$, the two branches of the pulse amplitude a_p exist for $p > p_* = 2/\sqrt{Y}$. In this case $a_p > 1/p$ and the effective (controlled) linear growth rate (supercriticality) $\mu = 1 - p \max_x |A| < 0$. Therefore, in this region of parameters the pulse tails are stable and a single pulse can exist in a large domain. For $Y < 0$, only one branch of the pulse amplitude, corresponding to the negative sign, exists for all $p > 0$. In this

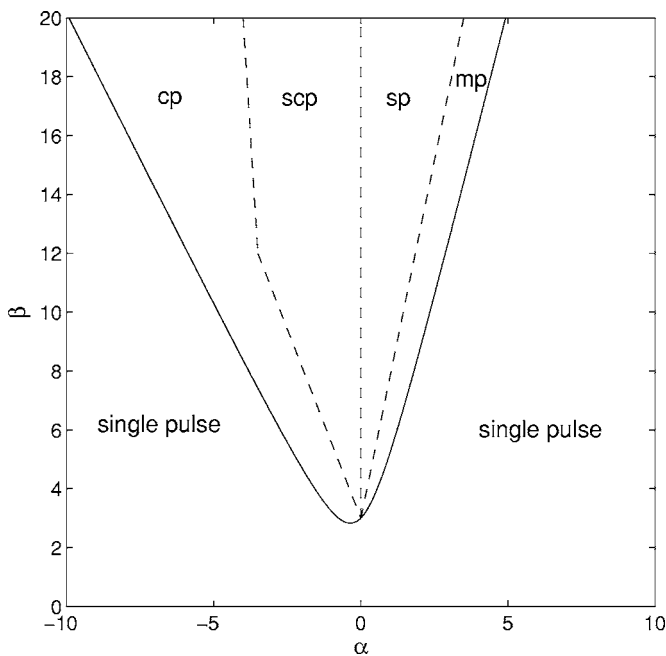


FIG. 1. “Phase diagram” of different nonlinear dynamic regimes described by Eq. (3). $Y > 0$: single pulse. $Y < 0$: “cp”—competing pulses, “scp”—short chaotic pulses, “sp”—synchronized pulses, “mp”—multiple pulses with stationary amplitude. The diagram is plotted for $p=5.0$ but it depends on p very weakly.

case, $a_p < 1/p$ and the effective supercriticality $\mu = 1 - p \max_x |A| > 0$; thus the tails of a pulse are unstable and a single localized pulse cannot exist in a large domain. Note that the sign of Y changes when its denominator passes through zero; at this boundary $a_p \rightarrow 1/p$. Thus, depending on the sign of Y , different dynamics is expected.

V. NUMERICAL SIMULATIONS

We have performed numerical simulations of the controlled CGLE (3) by means of a pseudospectral method with periodic boundary conditions, starting from small-amplitude random initial data with zero average. “Phase diagram” in (α, β) plane, showing different types of nonlinear dynamics exhibited by the solutions of Eq. (3) in (α, β) is presented in Fig. 1. Solid line corresponds to the values of α and β for which the denominator of Y is zero. Note that the system is invariant with respect to the transformation $\alpha \rightarrow -\alpha$, $\beta \rightarrow -\beta$, $\arg A \rightarrow -\arg A$; therefore, we consider only $\beta > 0$.

For the parameters α and β corresponding $Y > 0$, we have observed the formation of a single localized pulse described by Eqs. (6) and (7) with the negative sign in (7) (stable branch). This pulse is shown in Fig. 2. The upper figure presents the space-time diagram of $\text{Re}(A)$ starting from small-amplitude random data and shows the formation of a stable pulse in which time oscillations of real and imaginary part of A are spatially localized. The two lower figures show $\text{Re}(A)$, $\text{Im}(A)$, $|A|$ as well as the local wave number, $\partial\theta/\partial x$, where $\theta = \arg(A)$, for an established pulse at a particular moment of time. In this pulse the amplitude and the phase are stationary while the real and imaginary parts of A are oscillating.

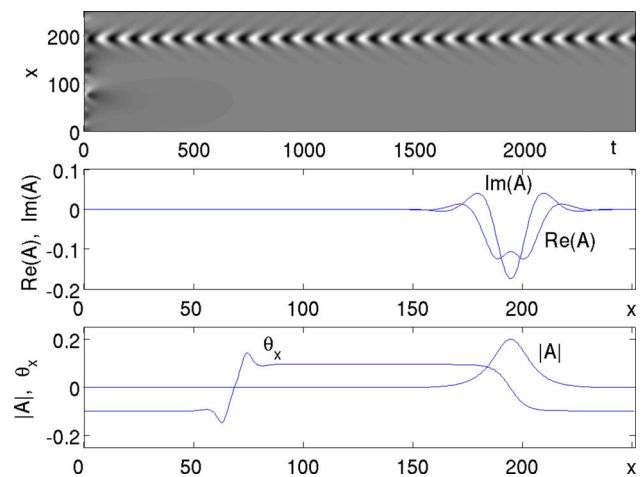


FIG. 2. (Color online) Numerical solution of Eq. (3) for $\alpha = -0.5$, $\beta = 2.0$, $p = 5.0$ corresponding to a single localized pulse described by the solution (6) and (7). Upper figure: spatiotemporal diagram of $\text{Re}(A)$ showing the pulse formation. Lower figures: $\text{Re}(A)$, $\text{Im}(A)$, $|A|$, and the local wave number, $\partial\theta/\partial x$ [$\theta = \arg(A)$], for an established pulse at a particular moment of time.

One can see that this pulse is a source of two rapidly decaying waves propagating away from the pulse, to the left and to the right; due to periodic boundary conditions, these two waves meet at some point in the domain and form a domain boundary (phase defect) corresponding to the abrupt jump of the wave number. Note that $\max(A) = 0.2016 > 1/p = 0.2$ for the parameter values corresponding to Fig. 2, so that the effective linear growth rate $\mu = 1 - p \max|A| < 0$; this makes the pulse tails stable and allows it to exist.

For the parameters α and β corresponding to $Y < 0$, when a single localized pulse is unstable, we have observed different types of behavior. For $\alpha < 0$ and (α, β) close to the left boundary where Y changes the sign we have observed the formation of competing pulses (region “cp” in Fig. 1), example of which is shown in Fig. 3. In this regime, a single pulse is born randomly in space and time, with the initial amplitude large enough so that the effective linear growth rate $\mu = 1 - p \max|A| < 0$ and all perturbations of the pulse tail get damped by the global control. Then the pulse amplitude decreases and gets stabilized at such value that $0 < \mu = 1 - p \max|A| \ll 1$ (for pulses shown in Fig. 3 $\mu = 0.06$). In this case, the tails of a single pulse are unstable but the instability growth rate is small so that the single pulse exists for a considerable time until the instability develops. The perturbations of the tails are growing and ultimately lead to the birth of another pulse, at a different location. The birth of another pulse, with large amplitude, damps all other perturbations in the domain by the global control, and the process repeats itself so that now the new pulse “rules” for some time, until the next “revolution” occurs and it gets “overthrown” by a new “ruler.”

For β fixed and α increasing, each single pulse in the competing pulses regime lasts shorter, and a few pulses can appear simultaneously. One observes a chaotic spatiotemporal dynamics of short pulses. This regime of short chaotic pulses is presented in Fig. 4(a) that shows spatiotemporal diagram of $|A|$. It is interesting that in this case each pulse is

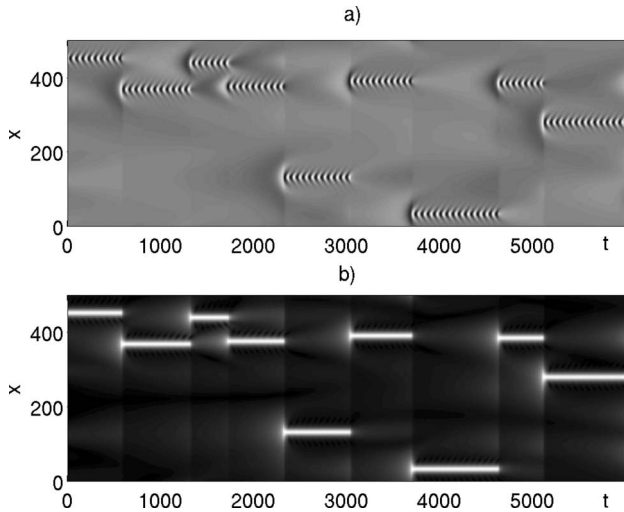


FIG. 3. Spatiotemporal diagram of a numerical solution of Eq. (3) for $\alpha=-0.5$, $\beta=3.0$, $p=5.0$, showing competing pulses: (a) $\text{Re}(A)$; (b) $|A|$.

characterized by a number of phase defects, domain boundaries between wave patterns characterized by different wave vectors, that manifest themselves as dark curves between the pulses. The regime of short chaotic pulses shown in Fig. 4(a) is observed for the parameter region “scp” in the phase diagram shown in Fig. 1. With the increase of the control parameter p the pulses become wider so that less pulses can occupy a given periodic domain. Note that somewhat similar short chaotic pulses were observed in the dynamics described by a subcritical cubic CGLE without control for certain values of the dispersion coefficients α and β [3,4], as well as in the dynamics of a CGLE with pure imaginary Landau coefficient (nonlinear dispersion only, without nonlinear saturation, [5]).

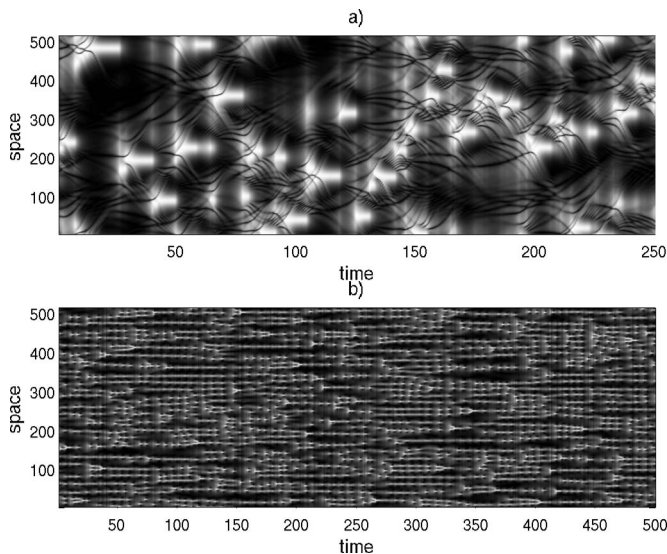


FIG. 4. Spatiotemporal diagram of numerical solutions of Eq. (3) showing (a) $|A|$ corresponding to the regime of spatiotemporally chaotic pulses, for $\alpha=-2.0$, $\beta=15.0$, $p=5.0$; (b) synchronized pulses, for $\alpha=1.0$, $\beta=10.0$, $p=5.0$.

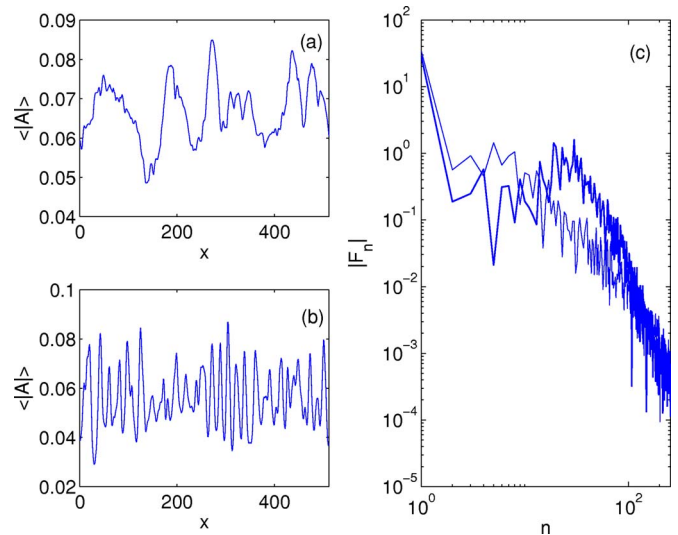


FIG. 5. (Color online) Time-averaged amplitude $\langle |A| \rangle$ corresponding to the regime of chaotic pulses (a) and spatially synchronized pulses (b) shown in Figs. 4(a) and 4(b), respectively; (c) Fourier power spectra of $\langle |A| \rangle$ shown in (a) (thin line) and (b) (thick line).

With further increase of α at fixed β , the short pulses start to synchronize so that the next new pulse appears more often at the same spatial location as its predecessor. A given pulse also lasts longer, and several pulses appearing at the same location form in a sense a long pulse with flickering amplitude. Spatiotemporal diagram showing such synchronized pulses is shown in Fig. 4(b). This regime is observed in the parameter region “sp” shown in Fig. 1.

Note that, as one can see in Fig. 4, when two pulses are born close enough to each other they interact and move towards each other, ultimately merging in a single pulse. It would be interesting to investigate the interaction of pulses in more detail, however, this is beyond the scope of the present paper. We shall study the interaction of pulses in future work.

The difference between the two regimes—spatiotemporally chaotic pulses and spatially synchronized pulses—can be also seen in Fig. 5. Figures 5(a) and 5(b) show the amplitude $\langle |A| \rangle$ averaged over a long time for the regime of chaotic pulses [Fig. 5(a)] and synchronized pulses [Fig. 5(b)]. One can see that while the pulse “spatial identity” is largely kept in the case of synchronized pulses, it is smeared out in time in the case of chaotic pulses. This can be clearly seen in Fig. 5(c) that presents the Fourier power spectra of $\langle |A| \rangle$ shown in Figs. 5(a) and 5(b) [thin line corresponds to Fig. 5(a) and thick line corresponds to Fig. 5(b)]. One can see that in the case of synchronized pulses the spectrum has a clear maximum corresponding to an average spatial period of the pulse spatial locations. The tails of the spectra for large wave numbers in both cases (a) and (b) obey power laws with the exponents -2.8 and -4.3 , respectively.

For α close to the right boundary of the region $Y < 0$, one observes the formation of multiple, coexisting pulses with stationary amplitude. The formation of such multiple pulses

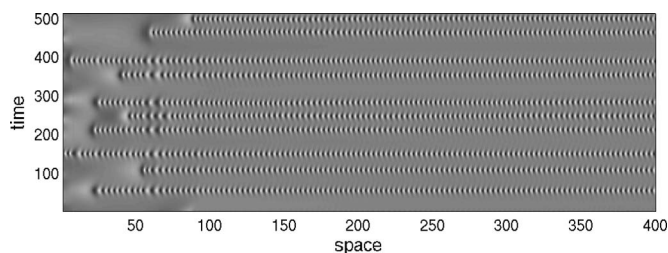


FIG. 6. Spatiotemporal diagram of a numerical solution of Eq. (3) for $\text{Re}(A)$, $\alpha=0.4$, $\beta=4.0$, $p=10$ showing the formation of co-existing pulses with stationary amplitude.

is shown in Fig. 6. With the decrease of the control parameter, each pulse becomes narrower, oscillates faster, the distances between the pulses decrease, and more pulses can occupy a given domain. The oscillation frequency of all pulses is the same and the phases are synchronized. The distances between the adjacent pulses are not the same but it cannot be too large due to instability of the pulse tail. Note that similar multipulse solutions were observed in the dynamics of a subcritical cubic CGLE without control in [3,4], for certain values of the parameters α and β .

VI. TWO-DIMENSIONAL CASE

It is interesting that the two types of nonlinear dynamics described above, a single localized pulse and competing pulses, are also observed in a *two-dimensional* system characterized by a long wave, subcritical oscillatory instability with the dispersion relation for the linear growth rate $\sigma(k) = \gamma + i\omega$, $\gamma = \gamma_R(R - R_c) - \delta k^2 + \dots$, $\omega = \omega_0 + \omega_2 k^2 + \omega_R(R - R_c) + \dots$, (where $k = |\mathbf{k}|$ is the absolute value of the perturbation wave vector), under the same global feedback control (1). The nonlinear dynamics of such a system is described by the following controlled two-dimensional CGLE:

$$A_t = A + (1 + i\alpha)\nabla^2 A + (1 + i\beta)|A|^2 A - pA \max|A|. \quad (8)$$

We have performed numerical simulations of Eq. (8) by means of a pseudospectral method starting from small-amplitude random noise. For some values of α and β we have observed the formation of a single localized pulse with stable tails ($\mu = 1 - p \max|A| < 0$); example of such pulse is shown in Fig. 7(a).

For some other parameter values we have observed the formation of competing pulses with $\mu > 0$ shown in Fig. 7(b). As in one-dimensional case, here a localized pulse appears with a large amplitude and damps other pulses due to the feedback control. However, since the established pulse amplitude is such that the effective linear growth rate of a trivial state is positive, the pulse tails are unstable; this leads to the growth of small perturbations leading to the formation of new pulses, and the process repeats itself in a chaotic manner.

VII. EFFECT OF DELAY

In this section we study the effect of possible feedback delay on the dynamics of a system exhibiting a subcritical

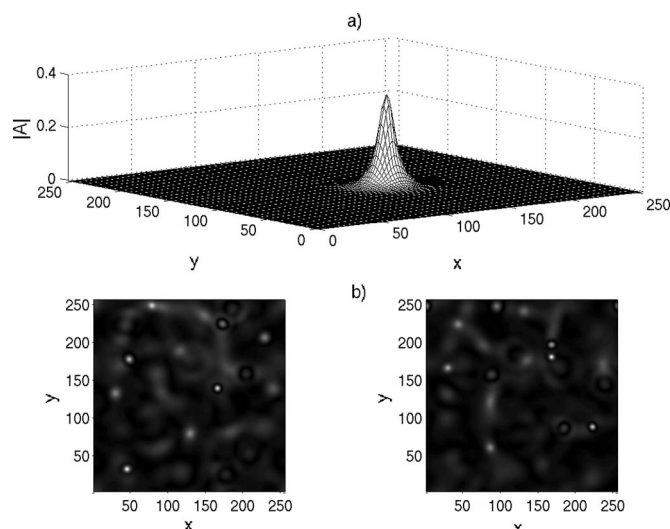


FIG. 7. Numerical solutions of Eq. (8) (absolute value $|A|$) in the form of (a) a spatially-localized pulse for $\alpha=5.0$, $\beta=5.0$, $p=3.0$; (b) competing, spatially-localized pulses for $\alpha=3.0$, $\beta=20.0$, $p=3.0$ shown at two different moments of time.

oscillatory instability. Thus we consider the feedback control with delay τ described by Eq. (2) so that the amplitude equation describing the system nonlinear dynamics under this feedback control will be

$$A_t = A + (1 + i\alpha)A_{xx} + (1 + i\beta)|A|^2 A - pA \max|A(t - \tau)|. \quad (9)$$

Obviously, the traveling wave solution (4) of Eq. (3) is also a solution of Eq. (9), and as before, it is always unstable. The localized pulse solution (6) and (7) is also a solution of Eq. (9) due to its stationary amplitude. However, the presence of delay can cause instability of a single localized pulse even in the region $Y > 0$ (see Fig. 1) where the effective supercriticality is negative, $\mu = 1 - p \max|A| < 0$. Also, the presence of delay can change the stability and behavior of other dynamic regimes described by the controlled CGLE and discussed above.

We have performed numerical simulations of Eq. (9) and investigated the effect of delay on the dynamic behavior. We have found that a single localized pulse described by (6) and (7) becomes oscillatory unstable when the feedback delay exceeds a critical value. The pulse amplitude, $|A|$, starts oscillating, with the oscillation amplitude increasing with the increase of the delay. The formation of such pulse, characterized by the oscillating amplitude, is shown in Fig. 8 that displays space-time diagrams of $|A|$ and $\text{Re}(A)$. One can see that the frequency of the pulse amplitude oscillations differs from the pulse own frequency of oscillations of $\text{Re}(A)$ and $\text{Im}(A)$. Thus, in the presence of the feedback delay above the critical value, $\text{Re}(A)$ and $\text{Im}(A)$ exhibit two-frequency oscillations. Also, the feedback-delay-induced oscillations are synchronized in space due to the global nature of control. Figure 9(a) presents the bifurcation diagram that shows how the amplitude of the delay-induced oscillations increases with the increase of the delay (the amplitude oscillations are

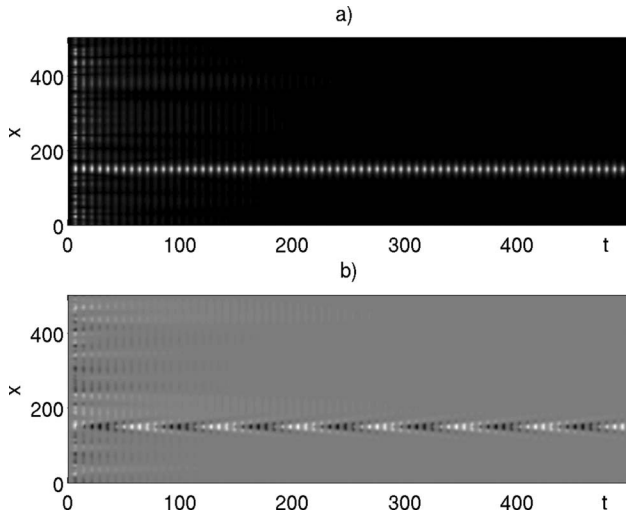


FIG. 8. Space-time diagrams of a numerical solution of Eq. (9) for $p=5.0$, $\alpha=-0.5$, $\beta=2.0$, and delay $\tau=1.5$ showing the formation of a localized pulse with an oscillating amplitude: (a) $|A|$; (b) $\text{Re}(A)$.

measured here in the center of the pulse). The critical value of the delay at which the stationary pulse becomes oscillatory unstable increases with the increase of the control parameter p ; this is shown in Fig. 9(b). Also, we have found that the delay critical value weakly depends on the parameters α and β .

The effect of the feedback delay on the regime of competing pulses is similar to its effect on a single localized pulse. We have found that when the delay exceeds a critical value the amplitude of the competing pulses starts oscillating in the same manner as that of a single localized pulse discussed above. Again, these feedback-induced oscillations are synchronized in space. This regime of competing pulses with oscillating amplitude is shown in Fig. 10. The critical delay at which the amplitude of the competing pulses undergoes the oscillatory instability is very close to that corresponding to a single localized pulse.

The effect of the feedback delay on other dynamic regimes described in the previous sections is also similar. After the delay increases above a critical value one observes glo-

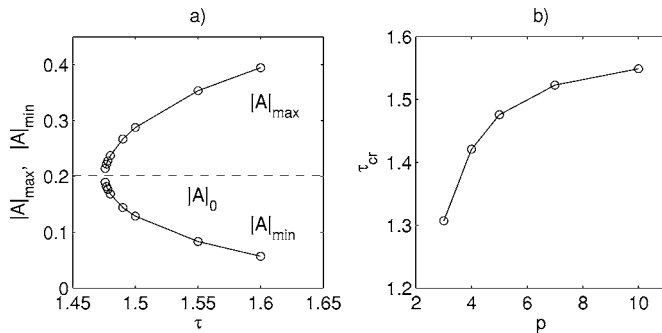


FIG. 9. (a) Maximum and minimum of the oscillating amplitude of a single localized pulse in its center as a function of the feedback delay τ for $p=5.0$, $\alpha=-0.5$, $\beta=2.0$; dashed line shows the constant amplitude of a localized pulse without delay. (b) Critical value of the feedback delay, τ_{cr} , as function of the control parameter p for the same values of α and β .

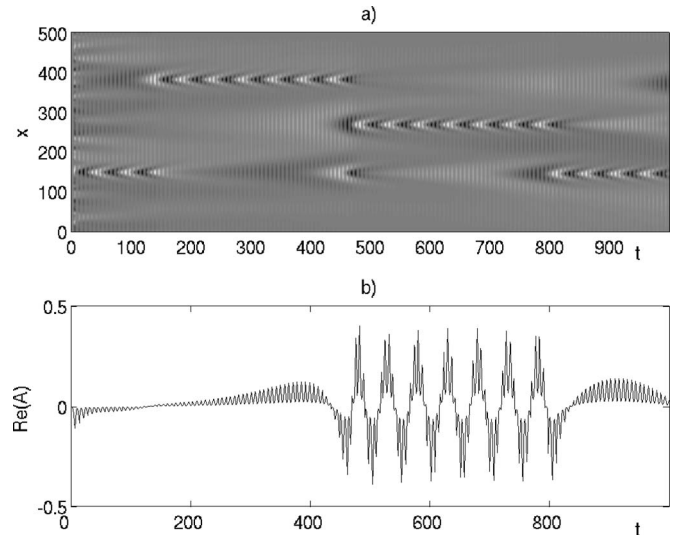


FIG. 10. Competing pulses with oscillating amplitude—numerical solution of Eq. (9) with $\alpha=-0.5$, $\beta=3.0$, $p=5.0$, $\tau=1.6$. (a) Spatiotemporal diagram of $\text{Re}(A)$. (b) Oscillations of $\text{Re}(A)$ in a particular point in space ($x=271$).

bal, spatially-synchronized oscillations of the amplitude of the pulses. Figure 11 shows feedback-delay-induced oscillations of the amplitudes in the regime of spatially-synchronized pulses [Fig. 11(a)] and in the regime of multiple pulses [Fig. 11(b); the formation of the multiple pulses with the oscillating amplitude is shown].

VIII. CONCLUSIONS

We have investigated the nonlinear dynamics of systems exhibiting a subcritical, short-wave oscillatory instability, under the action of a global feedback control based on the modulation of the bifurcation parameter as described by Eq.

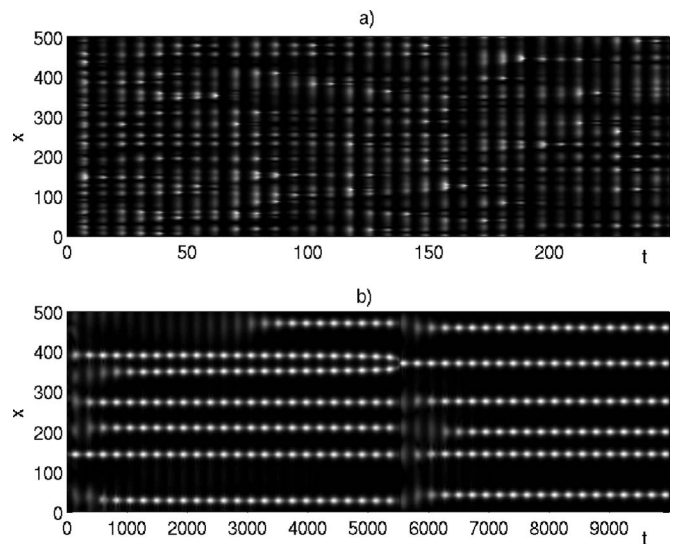


FIG. 11. Spatiotemporal diagrams of $|A|$ corresponding to a numerical solution of Eq. (9) for (a) $\alpha=1.0$, $\beta=10.0$, $p=5.0$, $\tau=1.5$, and (b) $\alpha=2.0$, $\beta=9.0$, $p=7.0$, $\tau=1.6$.

(1) or (2). The system nonlinear dynamics is described by the controlled CGLE (3) or (9), respectively. We have shown that this feedback control can prevent the blow up and sustain the system dynamics in the weakly nonlinear regime. We considered two cases: when the feedback delay can be neglected [Eq. (3)] and when it is significant [Eq. (9)]. For the case without delay we have shown that traveling wave solutions of Eq. (3) are unstable but the system can exhibit spatially-localized solutions in the form of pulses. We have found analytical solution of Eq. (3) in the form of a localized single pulse with stationary amplitude described by (6) and (7) that exists for certain values of the dispersion coefficients α and β . We have also found other dynamic regimes described by the controlled CGLE (3): competing pulses, chaotic pulses, synchronized pulses, as well as multiple pulses with stationary amplitude. The phase diagram of different regimes is shown in Fig. 1. We have also numerically studied the two-dimensional analog of Eqs. (3)–(8), that describes the weakly nonlinear dynamics of a system that exhibits long-wave subcritical oscillatory instability. We have found that solutions of Eq. (8) can exhibit similar nonlinear dynamics in the form of spatially-localized pulses with a constant amplitude, like oscillons, as well as competing spatially-localized pulses that appear at different locations, suppress all perturbations around them, but after some time get themselves replaced by new pulses appearing at a different location.

We have also investigated the effect of delay of the feedback control on the nonlinear dynamics of a system exhibiting a subcritical oscillatory instability and described by Eq.

(9). We have found that if the delay is small, the system dynamics is the same as that described by Eq. (3) without delay. If the delay exceeds a critical value, that depends on the control parameter p and weakly depends on the dispersion coefficients α and β , the amplitude of the pulses in all regimes described by the phase diagram shown in Fig. 1 exhibits oscillations whose amplitude increases with the increase of the delay. When the delay time exceeds the value equal to the blow up time of a system without control, that depends on the amplitude of the initial conditions, the system that starts its evolution from small-amplitude random noise blows up.

The obtained results demonstrate that the global feedback control of a system exhibiting a subcritical oscillatory instability, based on the feedback loop between the bifurcation parameter and the maximal perturbation amplitude and described by Eq. (1), is capable of stabilizing the system in the weakly nonlinear regime and can lead to an interesting nonlinear dynamics. Especially interesting, from experimental point of view, seems to be the possibility of the formation of spatially-localized single pulses (oscillons). These pulses, by choosing appropriate initial conditions, can be forced to form at a given location in space which opens an interesting opportunity to control pattern formation in systems exhibiting oscillatory dynamics, especially biological and chemical ones.

ACKNOWLEDGMENTS

This work was supported by the US NSF Grant No. DMS-0505878. A.A.N acknowledges the support of the Japan-Technion Society Research Fund.

-
- [1] M. C. Cross and P. C. Hohenberg, *Rev. Mod. Phys.* **65**, 851 (1993).
 - [2] I. S. Aranson and L. Kramer, *Rev. Mod. Phys.* **74**, 99 (2002).
 - [3] W. Schöpf and L. Kramer, *Phys. Rev. Lett.* **66**, 2316 (1991).
 - [4] S. Popp, O. Stiller, E. Kuznetsov, and L. Kramer, *Physica D* **114**, 81 (1998).
 - [5] C. S. Bretherton and E. A. Spiegel, *Phys. Lett.* **96**, 152 (1983).
 - [6] J. Tang and H. H. Bau, *Phys. Rev. Lett.* **70**, 1795 (1993).
 - [7] P. K. Yuen and H. H. Bau, *J. Fluid Mech.* **317**, 91 (1996).
 - [8] L. E. Howle, *Phys. Fluids* **9**, 1861 (1997).
 - [9] J. Tang and H. H. Bau, *J. Fluid Mech.* **363**, 153 (1998).
 - [10] H. H. Bau, *Int. J. Heat Mass Transfer* **42**, 1327 (1999).
 - [11] A. C. Or *et al.*, *J. Fluid Mech.* **387**, 321 (1999).
 - [12] A. C. Or and R. E. Kelly, *J. Fluid Mech.* **440**, 27 (2001).
 - [13] R. O. Grigoriev, *Phys. Fluids* **14**, 1895 (2002); **15**, 1363 (2003).
 - [14] T. Sakurai *et al.*, *Science* **296**, 2009 (2002).
 - [15] E. Mihaliuk *et al.*, *Phys. Rev. E* **65**, 065602(R) (2002).
 - [16] V. K. Vanag, A. M. Zhabotinsky, and I. R. Epstein, *J. Phys. Chem. A* **104**, 11566 (2000).
 - [17] I. R. Epstein, *ACS Symp. Ser.* **827**, 103 (2002).
 - [18] D. Lebedz and U. Brandt-Pollmann, *Phys. Rev. Lett.* **91**, 208301 (2003).
 - [19] M. Bertram and A. S. Mikhailov, *Phys. Rev. E* **63**, 066102 (2001); **67**, 036207 (2003).
 - [20] C. Beta, M. Bertram, A. S. Mikhailov, H. H. Rotermund, and G. Ertl, *Phys. Rev. E* **67**, 046224 (2003).
 - [21] T. V. Savina *et al.*, *J. Cryst. Growth* **240**, 292 (2002).
 - [22] A. A. Nepomnyashchy *et al.*, *Physica D* **199**, 61 (2004).
 - [23] D. Battogtokh and A. Mikhailov, *Physica D* **90**, 84 (1996).
 - [24] D. Battogtokh, A. Preusser, and A. Mikhailov, *Physica D* **106**, 327 (1997).
 - [25] Y. Kawamura and Y. Kuramoto, *Phys. Rev. E* **69**, 016202 (2004).
 - [26] B. Echebarria and A. Karma, *Chaos* **12**, 923 (2002).
 - [27] K. A. Montgomery and M. Silber, *Nonlinearity* **17**, 2225 (2004).
 - [28] P. Kolodner and G. Flätgen, *Phys. Rev. E* **61**, 2519 (2000).
 - [29] L. M. Hocking and K. Stewartson, *Proc. R. Soc. London, Ser. A* **326**, 289 (1972); N. R. Pereira and L. Stenflo, *Phys. Fluids* **20**, 1733 (1977); K. Nozaki and N. Bekki, *J. Phys. Soc. Jpn.* **53**, 1581 (1984); H. Chate and P. Manneville, *Phys. Lett. A* **171**, 183 (1992).
 - [30] J. Lega, *Physica D* **152**, 269 (2001).
 - [31] S. Fauve and O. Thual, *Phys. Rev. Lett.* **64**, 282 (1990).
 - [32] P. Marcq, H. Chate, and R. Conte, *Physica D* **73**, 305 (1994).